NEOPLASIA
www.neoplasia.com

Volume 22 Number 11 November 2020 pp. 606–616

Breast cancer cell debris diminishes therapeutic efficacy through heme oxygenase-1-mediated inactivation of M1-like tumor-associated macrophages

Seung Hyeon Kim [a,b]; Soma Saeidi [b,c]; Xiancai Zhong [b]; Shin-Young Gwak [b,c]; Ishrat Aklima Muna [b]; Sin-Aye Park [d]; Seong Hoon Kim [b]; Hye-Kyung Na [e]; Yeonsoo Joe [f]; Hun Taeg Chung [f]; Kyoung-Eun Kim [g]; Wonshik Han [g]; Young-Joon Surh [a,b,c,*]

[a] Cancer Research Institute, Seoul National University, Seoul 03087, South Korea; [b] Tumor Microenvironment Global Core Research Center, College of Pharmacy, Seoul National University, Seoul 08826, South Korea; [c] Department of Molecular Medicine and Biopharmaceutical Sciences, Graduate School of Convergence Science, Seoul National University, Seoul 08826, South Korea; [d] Department of Biomedical Laboratory Science, College of Medical Sciences, Soonchunhyang University, Asan 31538, South Korea; [e] Department of Food Science and Biotechnology, College of Knowledge-based Services Engineering, Sungshin Women's University, Seoul 01133, South Korea; [f] Department of Biological Sciences, University of Ulsan, Ulsan 44610, South Korea; [g] Department of Surgery, Seoul National University College of Medicine, Seoul 03087, South Korea

Abstract

Chemotherapy is commonly used as a major therapeutic option for breast cancer treatment, but its efficacy is often diminished by disruption of patient's anti-tumor immunity. Chemotherapy-generated tumor cell debris could hijack accumulated tumor-associated macrophages (TAMs), provoking tumor recurrence. Therefore, reprogramming TAMs to acquire an immunocompetent phenotype is a promising strategy to potentiate therapeutic efficacy. In this study, we analyzed the proportion of immune cells in the breast cancer patients who received chemotherapy. To validate our findings *in vivo*, we used a syngeneic murine breast cancer (4T1) model. Chemotherapy generates an immunosuppressive tumor microenvironment in breast cancer. Here, we show that phagocytic engulfment of tumor cell debris by TAMs reduces chemotherapeutic efficacy in a 4T1 breast cancer model. Specifically, the engulfment of tumor cell debris by macrophages reduced M1-like polarization through heme oxygenase-1 (HO-1) upregulation. Conversely, genetic or pharmacologic inhibition of HO-1 in TAMs restored the M1-like polarization. Our results demonstrate that tumor cell debris-induced HO-1 expression in macrophages regulates their polarization. Inhibition of HO-1 overexpression in TAMs may provoke a robust anti-tumor immune response, thereby potentiating the efficacy of chemotherapy.

Neoplasia (2020) 22 606–616

Keywords: Breast cancer, Chemotherapy, Tumor-associated macrophages, Phagocytosis, Tumor cell debris, Heme oxygenase-1

Abbreviations: TAMs, tumor-associated macrophages, HO-1, heme oxygenase-1, TME, tumor microenvironment, PTX, Paclitaxel, ZnPP, zinc protoporphyrin IX, BMDMs, bone marrow-derived macrophages, PS, phosphatidylserine, KO, knockout, LAP, LC3-associated phagocytosis, WT, wild-type

* Corresponding author: College of Pharmacy, Seoul National University, 1 Gwanak-ro, Gwanak-gu, Seoul 08826, South Korea.
e-mail address: surh@snu.ac.kr (Y.-J. Surh).

https://doi.org/10.1016/j.neo.2020.08.006

Introduction

Breast cancer, one of the most commonly diagnosed malignancies in women worldwide, is often treated with chemotherapy [1]. After chemotherapy, however, unwanted host effects provoke tumor recurrence and increase cancer cell aggressiveness, often via disruption of the patient's immune system [2,3]. The response to chemotherapy is affected by the tumor microenvironment (TME), which is the complex niche where cancer cells interact with the tumor stroma [4,5]. Chemotherapy can alter the proportion and activity of immune cells, including $CD8^+$ cytotoxic T lymphocytes that play major roles in reducing cancer progression [6–8]. Accordingly, potentiating the functional activity of cytotoxic lymphocytes, including $CD8^+$ T cells, has become a central goal of many anti-tumor therapies. One example of this is the combined use of chemotherapeutic agents plus immune-stimulators that target anti-tumor immunity [5].

The number of tumor-associated macrophages (TAMs) infiltrated into tumors is increased following chemotherapy [9]. TAMs, which act as a bridge between innate and adaptive immunity, could potentially be targeted to complement chemotherapeutic efficacy [10]. Notably, TAMs have dual roles in cancer development and progression [10]: those associated with poor clinical outcome display the M2-like macrophage (alternatively activated) phenotype which promotes tumor progression through immunosuppression [10], whereas those induced by local signals display the M1-like macrophage (classically activated) phenotype associated with cytotoxic and T-cell-mediated anti-tumor activities [10,11]. Recent studies have focused on the modulation of signaling factors and events to skew TAMs toward M1-like TAMs for enhancing the host anti-tumor response [12–14].

For decades, anti-cancer therapies have been primarily intended to destroy cancer cells to reduce tumor growth [15,16]. When such therapies kill tumor cells, tumor cell debris (apoptotic cells, necrotic cells and cell fragments) can be generated and released to the surrounding area [15]. Importantly, the tumor cell debris generated by chemotherapy can contribute to accelerating tumor growth [15,17]. Macrophages critically remove dead cells [18,19], and their phagocytosis of apoptotic cancer cells has been suggested to promote tumor growth by modulating TAM activity [20–22]. However, the molecular mechanisms underlying the interaction between tumor cell debris and TAMs remain largely unresolved.

Chemotherapy-induced oxidative stress is one mechanism by which cancer cells are killed [23]. However, cancer cells can bypass oxidative cell death by activating their anti-oxidant defense system [23–25]. The overexpression of stress-responsive antioxidative enzyme, heme oxygenase-1 (HO-1) was reported to be associated with poor prognosis in breast cancer patients receiving chemotherapy [24,26]. Conversely, HO-1 inactivation can promote the effectiveness of anti-cancer therapy to inhibit tumor growth [26–29]. Recent studies suggest that the induction of HO-1 in TAMs plays an important role in cancer progression [26,30,31]. However, the role of overexpressed HO-1 in TAMs during chemotherapy remains poorly understood. Here we report that breast tumor cell debris-induced HO-1 expression in TAMs can diminish the efficacy of paclitaxel (PTX), a representative anticancer drug frequently used for the treatment of breast cancer.

Materials and methods

Human study

This study was approved by the institutional review board (IRB) of Seoul National University Hospital (Seoul, South Korea), and all patients provided signed informed consent for collection of specimens (IRB number: 1807-061-957). The tumor specimens were kindly supplied by Prof. Wonshik Han of Seoul National University Hospital.

Animal study

Balb/c mice (6 ~ 9 weeks old) were purchased from Orient Bio (Gyeonggi-Do, South Korea). HO-1 KO mice, in which the HO-1 gene was deleted by targeted gene knockout, were kindly provided by Dr. M.A. Perrella (Harvard Medical School, Boston, MA, USA). 4T1 murine mammary adenocarcinoma cells (1×10^5) were subcutaneously implanted in the mammary glands of female Balb/c mice as previously described [32]. Tumors were grown for 10 days before mice were injected with PTX. The tumor size was measured by caliper (width × length × height × 0.52 = mm^3). All the animals were maintained according to the relevant institutional animal care guidelines. Animal experimental procedures were approved by the institutional animal care and use committee at Seoul National University, South Korea (IACUC number: SNU-170710-2)

Cell culture

To generate primary bone marrow-derived macrophages (BMDMs), we obtained bone marrow cells by flushing the long bones of mice (6 ~ 12 weeks old). Bone marrow cells were plated in DMEM supplemented with 10% fetal bovine serum (FBS; Gibco, #16000-044), 100 μg/ml streptomycin, 100 U/ml penicillin and 20 ng/ml M-CSF (Biolegend, #576406) and cultured for 7 days to allow for macrophage differentiation. Murine 4T1 cells were purchased from the American Type Culture Collection (ATCC) and cultured in DMEM supplemented with 10% FBS, 100 μg/ml streptomycin and 100 U/ml penicillin. Cells were maintained at 37 °C in a humidified atmosphere of 5% CO_2.

Macrophage polarization

To generate M1-like polarized macrophages, BMDMs were incubated with 100 ng/ml of lipopolysaccharide (LPS; Sigma, #L2630) for 24 h as previously described [14].

Generation of tumor cell debris

Tumor cell debris was generated by incubating breast cancer cells (1×10^7) in medium supplemented with PTX (1 mM) for 24 h. The presence of dead cells among the debris was confirmed by the annexin V/propidium iodide (PI) assay.

Isolation of single cells from mouse tumors

Tumors were collected from mice and dissociated into single cells as described previously [33]. Specifically, tumor implanted mice were euthanized and tumors were harvested. Tumors were then minced and mechanically disaggregated. The disaggregated tumors were then passed through a 40 μm filter using DMEM supplemented with 2% FBS to prepare a single cell suspension.

Flow cytometric analysis

Single-cell suspensions were washed with phosphate-buffered saline (PBS) containing 1% FBS and non-specific antibody binding was blocked with anti-mouse CD16/32 Fc receptor block antibody (Biolegend #101319). The cells were then stained by incubation on ice for 30 min with the following fluorescence-conjugated antibodies: anti-mouse CD45 APC (clone I3/2.3, Biolegend #147708), anti-mouse F4/80 PerCP/Cy5.5 (clone BM8, Biolegend #123128), anti-mouse F4/80 APC (clone BM8, Biolegend #123116), anti-mouse CD3ε Alexa Fluor 700 (clone 500A2, Biolegend #152316), anti-mouse CD8a PE/Cy7

(clone 53-6.7, Biolegend #100722), anti-mouse CD206 FITC (clone C068C2, Biolegend #141704). The cells were washed with PBS and subjected to flow cytometry. Dead cells were excluded by 4′,6-diamidino-2-phenylindole (DAPI; Thermo Fisher Scientific, #D1306) staining.

For intracellular staining, cells were fixed and permeabilized with a fixation/permeabilization buffer set (Thermo Fisher Scientific, #00-5521-00), and then stained with the following antibodies: anti-mouse IL-12p40 PE (clone C15.6, Biolegend #505204), anti-mouse TNF-α FITC (clone MP6-XT22, Biolegend #506304).

To examine the presence of EpCAM as an intracellular marker of breast tumor cell debris, cells were fixed with 2% formaldehyde in PBS for 30 min at room temperature, permeabilized with 0.1% Tween-20 in PBS for 15 min at room temperature, and stained with anti-mouse EpCAM FITC (clone G8.8, Biolegend #118208). We used FACS Calibur, LSR Fortessa X-20 and FACS Aria III (BD) machines for the above-listed analyses. All samples were analyzed using the Flow jo software package (Tree Star).

Cell sorting

Single-cell suspensions obtained from tumors were stained with DAPI, anti-CD45 APC (clone I3/2.3, Biolegend #147708) and anti-CD11b Alexa Fluor700 (clone M1/70, Biolegend #101222) and subjected to FACS using a FACS Aria III (BD). Live cells were identified as DAPI negative and TAMs as $CD45^+$ $CD11b^+F4/80^+$ populations.

Immunofluorescence

Tumor specimens were fixed, paraffin-embedded and sectioned. The sections were deparaffinized and rehydrated by serial washes with graded xylene and alcohol. For immunofluorescence staining, tissue sections were boiled in 10 mM sodium citrate (pH 6), subjected to serial washing, blocked with 5% FBS in PBST (PBS + 0.1% Tween 20) and co-stained with HO-1 (Enzo, #ADI-OSA-111-D), CD8 Alexa Fluor 594 (clone RPA-T8, Biolegend #301056), CD11b Alexa Fluor 488 (clone M1/70, Biolegend #101217), CD206 (clone 15-2, Biolegend #321101), epidermal growth factor receptor (EGFR; Santa Cuz #sc-03G) or epithelial cell adhesion molecule EpCAM (Santa Cuz #sc-25308) and DAPI (Thermo Fisher Scientific) overnight at 4 °C. To analyze the phagocytosis of macrophages, the isolated myeloid cells were incubated with F4/80 (Santa Cruz). The resulting $CD11b^+$ $F4/80^+$ cells were dispensed to glass slides, permeabilized for 5 min at room temperature using 0.2% Triton X-100 in PBS and blocked with 3% bovine serum albumin (BSA) in PBS containing 0.1% Triton X-100 for 1 h at room temperature. Anti-mouse EpCAM Alexa Fluor 594 (clone G8.8, Biolegend #118222) was used to stain tumor cell debris engulfed in macrophages. To assess the expression of HO-1 in macrophages, myeloid cells were incubated with F4/80 (Santa Cruz), permeabilized, stained with HO-1 (Enzo #ADI-OSA-111-D) and incubated with the appropriate secondary antibodies. Nuclei were counterstained with DAPI and immunofluorescence images were collected on a Zeiss LSM 710 confocal microscope (Zeiss).

Quantitative PCR (qPCR)

Total RNA was isolated from cells and tumor tissues using the TRIzol™ reagent (Invitrogen) according to the manufacturer's instructions and reverse transcribed using Moloney murine leukemia virus reverse transcriptase (Promega). qPCR analysis was performed using a 7300 Real-Time PCR System (Thermo Fisher Scientific). Gene expression data are presented after normalization with an internal control. The following primers were utilized:

Gene symbol	Primer sequences
Il10	Forward: GCTCTTACTGACTGGCATGAG Reverse: CGCAGCTCTAGGAGCATGTG
Tnf	Forward: CCCTCACACTCAGATCATCTTCT Reverse: GCTACGACGTGGGCTACAG
Il12b	Forward: TGGTTTGCCATCGTTTTGCTG Reverse: ACAGGTGAGGTTCACTGTTTG
Actb	Forward: TGCTAGGAGCCAGAGCAGTA Reverse: AGTGTGACGTTGACATCCGT

Western blot analysis

Whole-cell lysates or tumor extracts were prepared by suspending the cells or tumor tissues in lysis buffer (Cell Signaling Technology) containing protease inhibitors (Roche) on ice, followed by centrifugation for 15 min at 13,000*g*. Protein concentrations were assessed by a BSA assay (Invitrogen). Proteins were resolved by sodium dodecyl sulfate polyacrylamide gel electrophoresis (SDS–PAGE) and transferred to PVDF membranes (Gelman Laboratory). The membranes were incubated with primary antibodies at 4 °C overnight, washed and incubated with horseradish peroxidase-conjugated secondary antibodies. The results were developed with ECL reagents (Amersham Pharmacia Biotech) according to the manufacturer's instructions and visualized using a LAS 4000 (Fujifilm Life Science).

Statistics

Data are presented as the mean þ SEM (standard error of the mean). For between-group differences in the mouse experiments, significance was determined using one-way ANOVA analysis with a Tukey's post hoc test. The Student's *t*-test was used to compare data from control and experimental conditions. The analyses were applied using SigmaPlot 12 (Systat Software).

Results

Chemotherapy facilitates the development of an immunosuppressive TME in breast cancer

Chemotherapy acts as a double-edged sword in the regulation of cancer progression [16,34]. Therapy-induced changes of the TME often abrogate treatment efficacy via unwanted host effects, such as modification of immune cell infiltration and increased production/secretion of immunosuppressive factors [4]. To assess the chemotherapy-associated changes in immune cell subsets, we measured the proportion of immune cells in the breast cancer patient who received chemotherapy. Immunofluorescence staining revealed that the number of intratumoral $CD8^+$ T lymphocytes (Fig. 1a) was reduced, while that of M2-like TAMs (identified by positivity for CD206) was increased in tumor tissues after chemotherapy (Fig. 1b).

Next, we examined the impact of cytotoxic therapy on anti-tumor immunity in the TME. For this purpose, we used a syngeneic murine breast cancer (4T1) model in which mice were treated with PTX, one of the most commonly used chemotherapeutic agents [29,35,36]. To determine whether PTX treatment altered the proportion of tumor-infiltrating immune cells, we analyzed infiltrating immune cells stained with fluorochrome-conjugated antibodies by flow cytometry [37]. We examined the proportion of $CD8^+$ cytotoxic T lymphocytes, which play

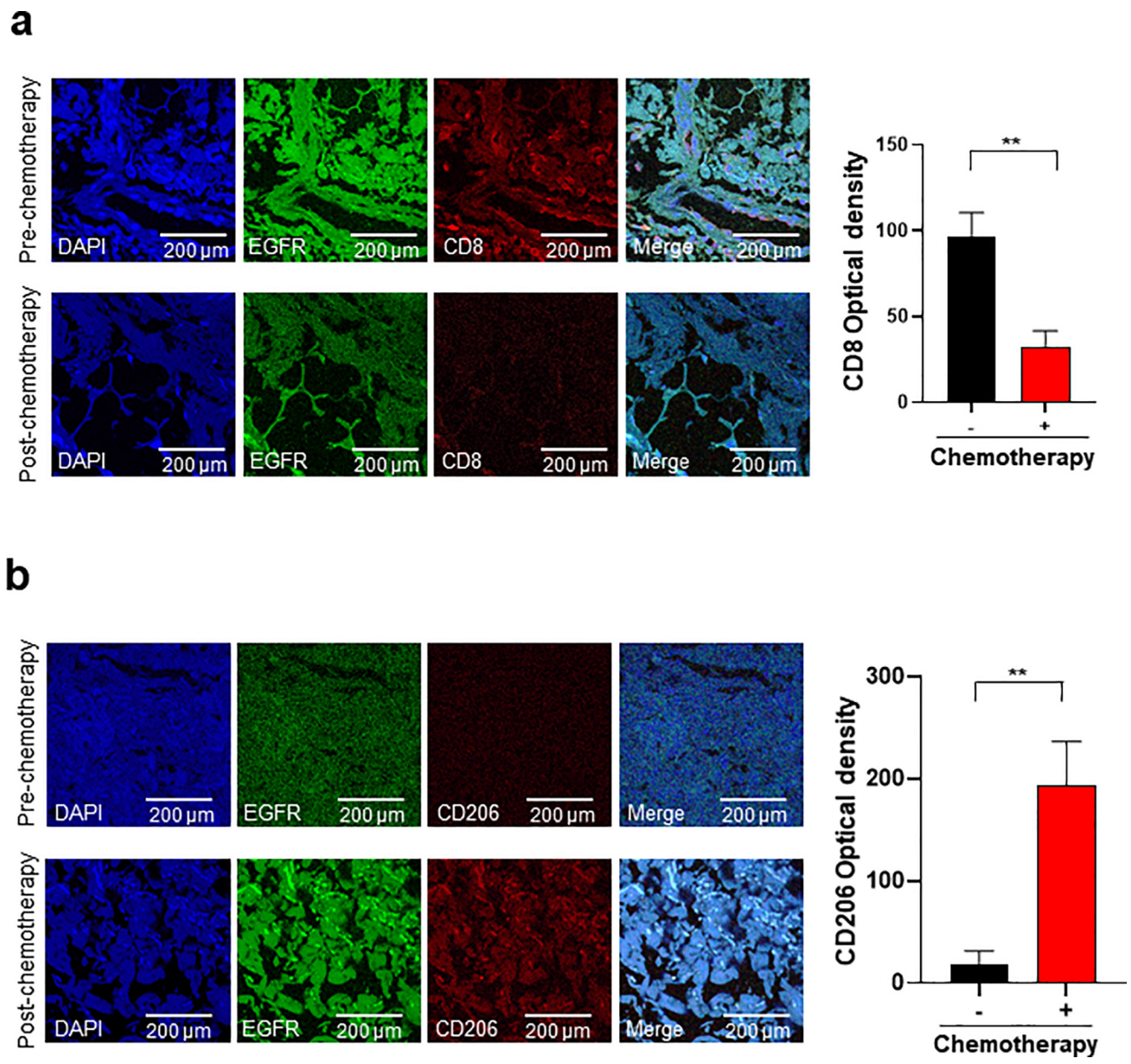

Fig. 1. Chemotherapy alters the proportion of tumor-infiltrating immune cells. (**a**) Representative images of tumor sections from the patients with breast cancer before and after chemotherapy, stained for the presence of $CD8^+$ cytotoxic T cells. The EGFR expression was measured as a cancer cell marker. (**b**) Representative images of tumor tissues from breast cancer patients receiving chemotherapy, stained for CD206, a marker for M2-like TAMs. $^{**}P < 0.01$.

a decisive role in suppressing tumor growth, and found that the percentage of recruited $CD8^+$ T cells was significantly reduced in the PTX-treated group (Fig. 2**a**).

Phagocytosis of tumor cell debris regulates the polarization of macrophages to a pro-tumor phenotype

Chemotherapy affects the polarization of TAMs in a way conferring immunosuppressive functions that suppress anti-tumor immunity [31,38,39]. To understand how PTX therapy alters the TAM phenotype, we considered the physiological events that characterize the TME after cytotoxic therapy. Given that macrophages function to clear tumor cell debris in the TME [18], we examined whether phagocytosis of the tumor cell debris generated by chemotherapy could contribute to TAM polarization. The proportion of macrophages phagocytosing breast tumor cell debris (identified by positivity for the breast cancer cell marker, $EpCAM^+$) was increased after PTX treatment (Fig. 2b). We observed that tumor cell debris ($EpCAM^+$) was engulfed by macrophages ($F4/80^+$ cells) from 4T1 tumor-bearing mice injected with PTX (Fig. 2c).

To investigate the role of tumor cell debris in the polarization of macrophages, we co-cultured BMDMs with 4T1 breast cancer cells treated with PTX for 24 h. PTX-induced cell death was confirmed by annexin V/PI staining. Notably, the mRNA levels of *Tnf* and *Il12b* were reduced in M1-like polarized BMDMs co-cultured with cancer cell debris (Fig. 2d, e). To investigate whether tumor cell debris could affect the polarization of macrophages to the M2-like phenotype, we examined the expression of the M2-like macrophage marker, CD206 in macrophages co-cultured with tumor cell debris or live breast cancer cells. The CD206 expression

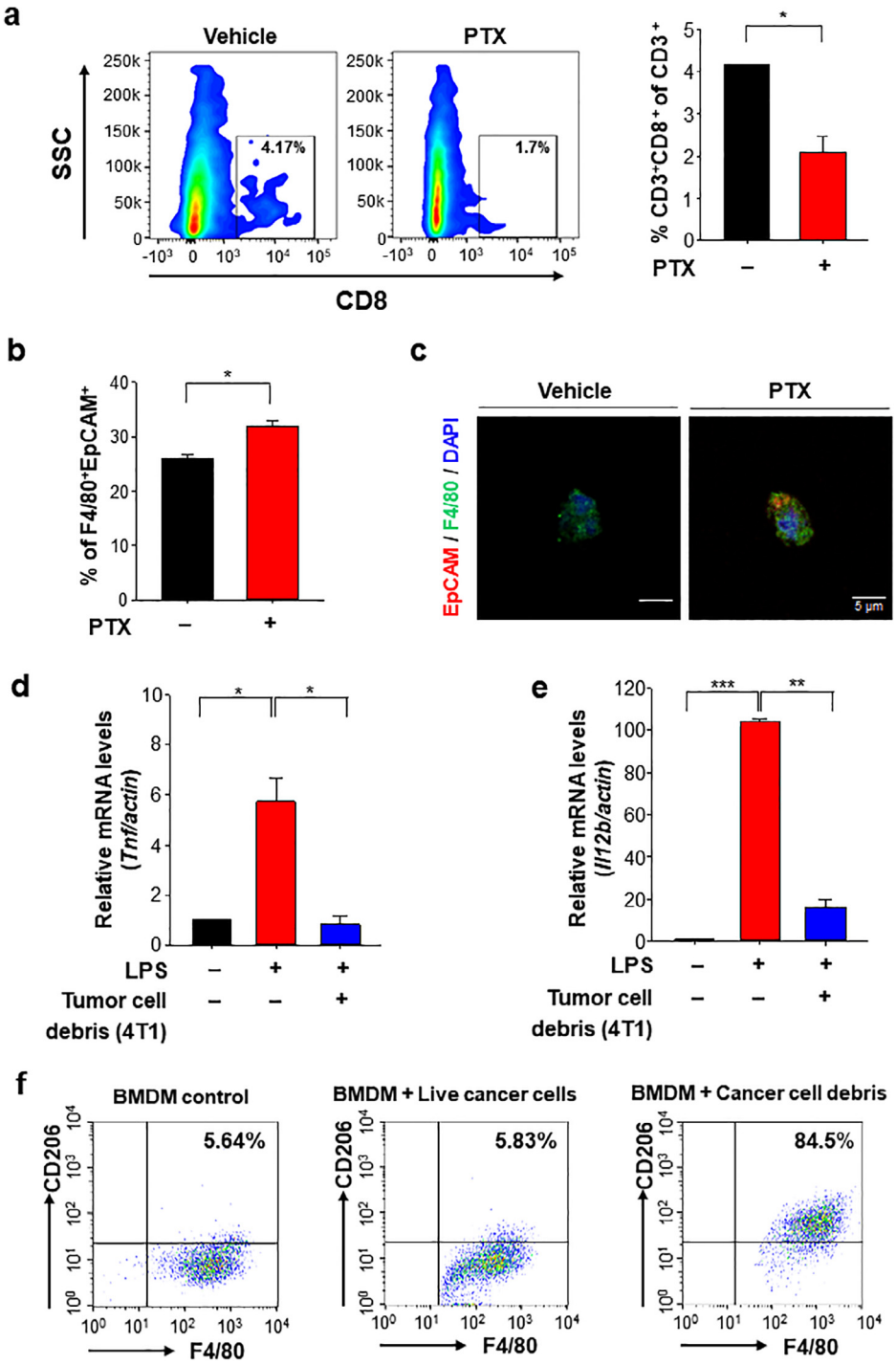

Fig. 2. Tumor cell debris formed during chemotherapy contributes to macrophage polarization. (**a**) Mice were implanted subcutaneously in the mammary gland with 4T1 tumor cells. At 10 days after tumor cell injection, the mice were subjected to intraperitoneal injection of vehicle or PTX (5 mg/kg) every 5 day. Mice were sacrificed on day 15 after PTX treatment, and tumors were collected. Effects of PTX on the proportion of $CD45^+CD3^+CD8^+$ tumor-infiltrating lymphocytes were analyzed. Whole tumors were dissociated into single cells and flow cytometry was used to identify tumor-infiltrating immune cells. The proportion of $CD45^+CD3^+CD8^+$ tumor-infiltrating lymphocytes in tumors collected from mice treated with or without PTX was assessed by flow cytometry. (**b**) Phagocytosis of breast tumor cell debris was analyzed as the proportion of macrophages found to contain intracellular EpCAM, as assessed by flow cytometry. (**c**) Whole tumors were processed into single cells. $CD45^+CD11b^+$ myeloid cells were isolated, cytospun onto glass slides, and subjected to immunofluorescence analysis for identification of breast tumor cell debris ($EpCAM^+$) phagocytosed by macrophages ($F4/80^+$). (**d**, **e**) BMDMs were treated with 100 ng/ml LPS for 24 h to cause them to skew toward the M1-like phenotype. The mRNA expression levels of *Tnf* (**d**) and *Il12b* (**e**) in the M1-like polarized macrophages treated with or without 4T1 cell debris for 30 h were measured by qPCR. (**f**) Macrophages were co-cultured with live 4T1 cells or 4T1 tumor cell debris for 24 h, and the CD206 expression of macrophages was analyzed by flow cytometry. The significance of differences between groups was determined by one-way ANOVA (Tukey's post hoc test) and the Student's *t*-test was used to compare results obtained from the control and experimental conditions. $^*P < 0.05$, $^{**}P < 0.01$, and $^{***}P < 0.001$.

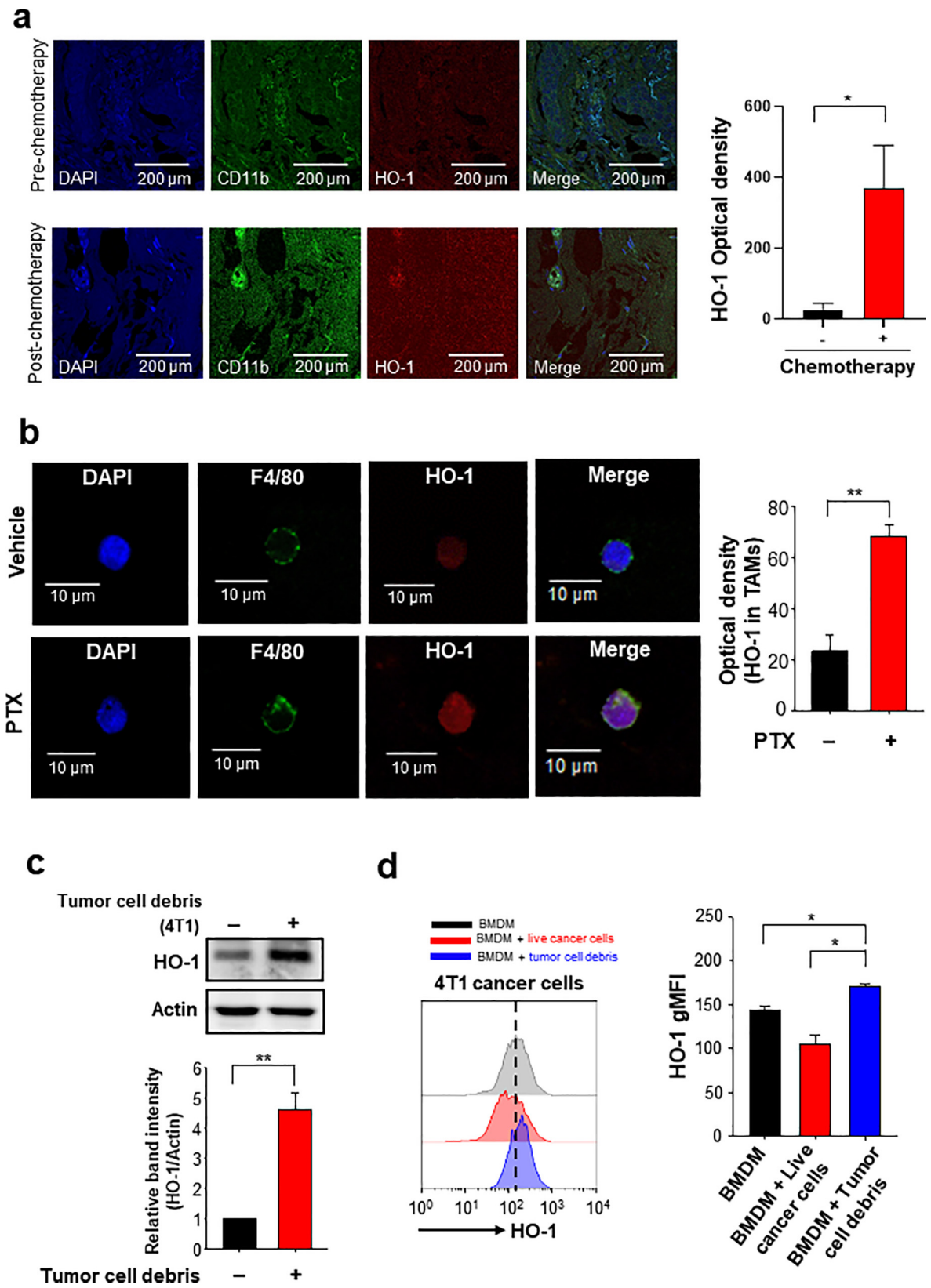

Fig. 3. Phagocytosis of tumor cell debris induces HO-1 expression in macrophages. (**a**) Representative images of CD11b and HO-1 expressed in tumor tissues from breast cancer patients before and after chemotherapy. (**b**) Representative immunofluorescence images of HO-1 expression in TAMs from 4T1 breast cancer-bearing mice. (**c**) The protein expression levels of HO-1 in macrophages co-incubated for 8 h with tumor cell debris generated from murine 4T1 measured by Western blot analysis. (**d**) The HO-1 expression levels of macrophages ($F4/80^+$) cultured with live cancer cells or tumor cell debris analyzed by flow cytometry. Comparisons between the control and experimental groups were performed with the Student's *t*-test. One-way ANOVA (Tukey's post hoc test) was used to determine the significance of differences between groups. $^*P < 0.05$ and $^{**}P < 0.01$.

levels of macrophages were higher in macrophages treated with tumor cell debris compared to those co-cultured with live breast cancer cells (Fig. 2f). Likewise, BMDMs co-incubated with breast tumor cell debris showed elevated mRNA levels of *Il10* which is an immunosuppressive M2-like marker (Supplemental Fig. S1a). These results suggest that engulfment of tumor cell debris causes an immunosuppression, which can be an important aspect of the TME changes seen in the wake of anti-cancer therapy.

Engulfment of tumor cell debris induces HO-1 expression in macrophages

Chemotherapy used for tumor eradication in breast cancer patients has been reported to upregulate HO-1 expression, which is associated with the low survival rate [23,26]). Moreover, TAMs represent the major tumoral source of HO-1 in breast cancer [26]. To determine whether HO-1

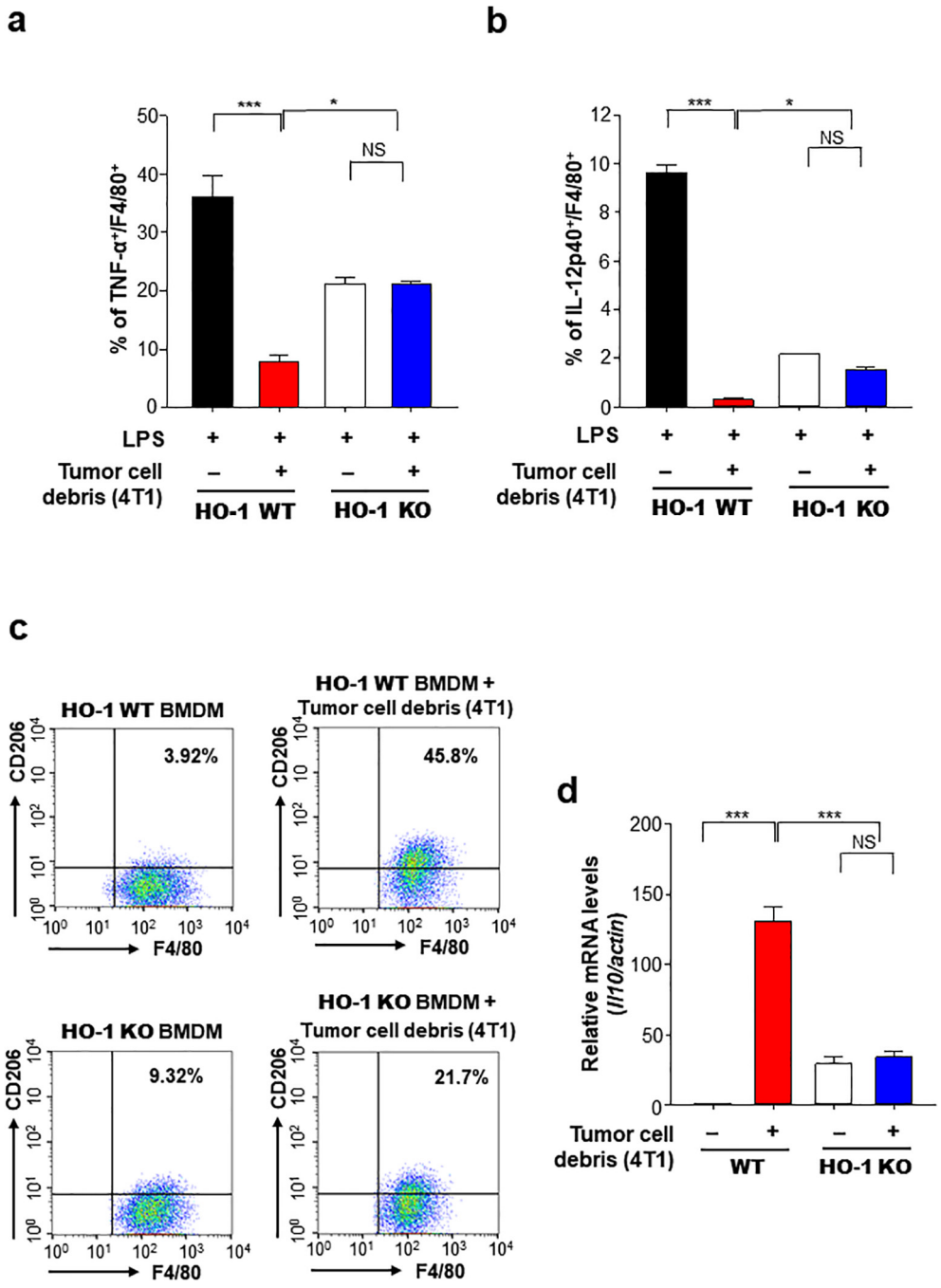

Fig. 4. HO-1 expression induced by is involved in the modulation of macrophage polarization. (**a**, **b**) BMDMs from WT or HO-1 KO mice were treated with LPS (100 ng/ml) for 24 h. The resulting M1-like polarized macrophages were co-cultured with 4T1 tumor cell debris for 30 h. The proportion of macrophages expressing TNF-α (**a**) and IL-12p40 (**b**) was determined by flow cytometry. (**c**) BMDMs from WT or HO-1 KO mice were co-treated with 4T1 tumor cell debris for 24 h, and the expression of CD206 in macrophages was analyzed by flow cytometry. (**d**) BMDMs from WT or HO-1 KO mice were co-cultured with or without 4T1 tumor cell debris for 8 h, and the mRNA levels of *Il10* were analyzed by qPCR. $^{*}P < 0.05$ and $^{***}P < 0.001$. NS: not significant.

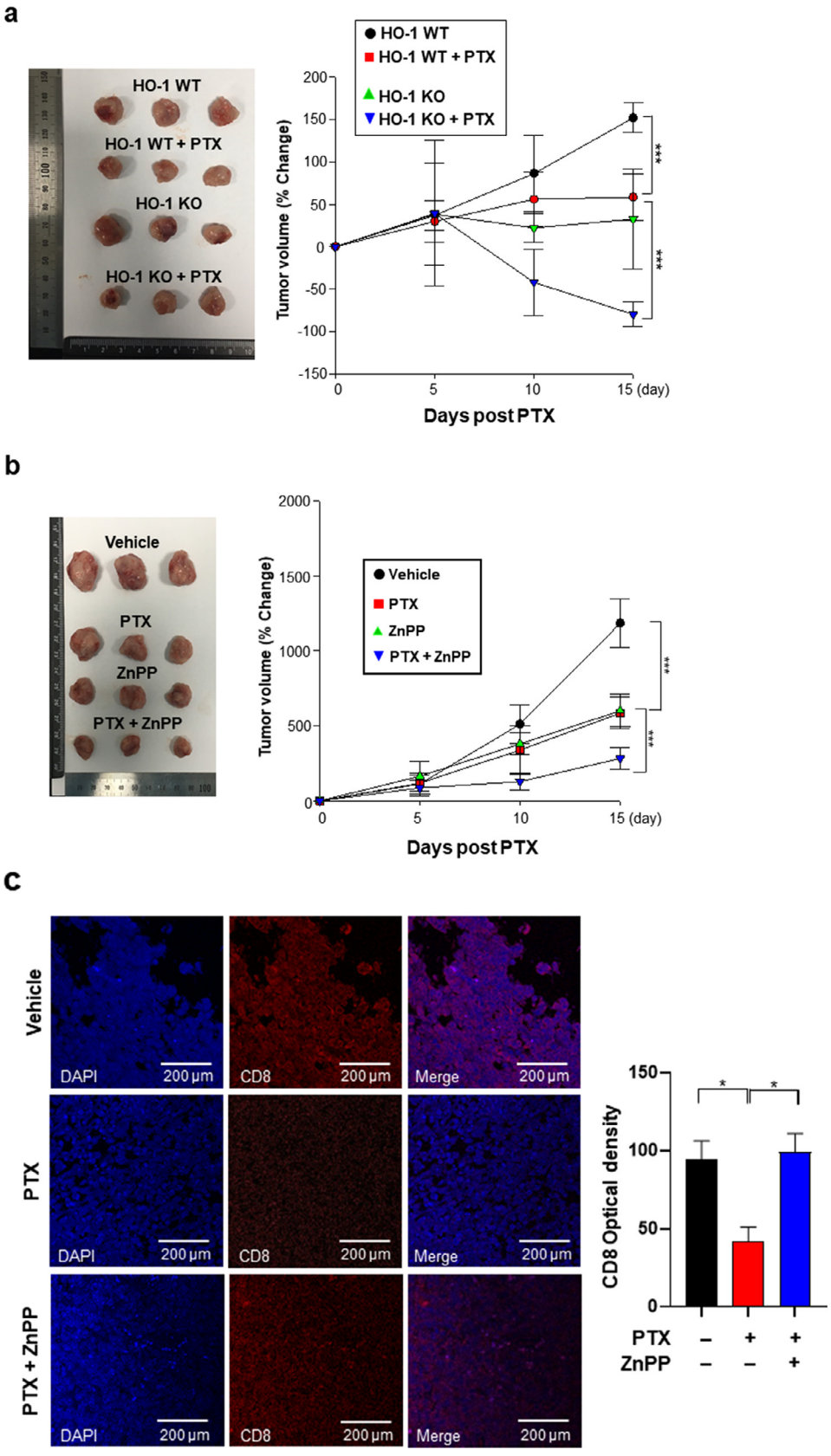

Fig. 5. Inactivation of HO-1 sensitizes the host response to PTX therapy. (**a**) WT or HO-1 KO mice implanted with 4T1 tumors were intraperitoneally injected with vehicle or PTX (5 mg/kg) for 5 days. Mice were killed on day 15 after PTX treatment, and tumors were collected. Tumor volume as a % change was calculated and plotted as the total mean þ SEM. (**b**) Mice implanted with 4T1 tumor cells received vehicle or PTX (5 mg/kg) for 5 days with or without daily intraperitoneal injection of ZnPP (40 mg/kg). Mice were sacrificed on day 15 after PTX treatment, and tumors were collected. Tumor volume was calculated as a relative change and plotted as the total mean þ SEM. (**c**) Representative images of tumor sections stained for $CD8^+$ T cells and DAPI are shown. The significance of the differences between experimental groups was determined using one-way ANOVA (Tukey's post hoc test). $^*P < 0.05$ and $^{***}P < 0.001$.

expression of TAMs was enhanced after chemotherapy, the HO-1 expression in macrophages in breast cancer patient samples collected before and after chemotherapy was measured. In macrophages of breast cancer patients following chemotherapy, overexpression of HO-1 was confirmed (Fig. 3a). The elevated expression of HO-1 in TAMs derived from 4T1 tumor-bearing mice injected with PTX was confirmed by immunofluorescence staining (Fig. 3b).

In another experiment, BMDMs co-cultured with tumor cell debris induced HO-1 expression to a greater extent than did the untreated group (Fig. 3c). To further determine whether tumor cell debris is critical for the overexpression of HO-1 in macrophages following chemotherapy, the expression levels of HO-1 in macrophages co-cultured with live breast cancer cells or PTX-generated tumor cell debris were compared. Macrophages co-incubated with breast cancer cell debris showed significantly higher levels of HO-1 than those co-cultured with live breast cancer cells (Fig. 3d).

HO-1 overexpression triggered by phagocytosis of tumor cell debris regulates the polarization of macrophage

Considering that HO-1 is an important factor for the polarization of macrophages, it could be a promising target in cancer immunotherapy [10,40]. To test whether the tumor cell debris-induced HO-1 overexpression in macrophages is essential for their polarization, we used HO-1-deficient BMDMs from HO-1 knockout (HO-1 KO) mice. First, we examined whether ablation of HO-1 could affect the activation of M1-like polarized macrophages treated with tumor cell debris. The proportion of M1-like macrophages, as assessed by the upregulated expression of TNF-α and IL-12p40, was significantly decreased in wild-type (WT) cells co-cultured with 4T1 tumor cell debris, whereas HO-1 KO macrophages were unaffected by this treatment (Fig. 4a, b). To further explore the role of HO-1 activity in macrophage polarization, we used zinc protoporphyrin IX (ZnPP), which is a pharmacologic inhibitor of HO-1. We found that the ZnPP-mediated inhibition of HO-1 activity restored the mRNA levels of *Tnf* and *Il12b* in M1-like polarized macrophages co-cultured with 4T1 tumor cell debris (Supplemental Fig. S1b, c).

Next, we examined whether inhibition of HO-1 activity could affect M2-like polarization. The expression of CD206 in HO-1-deficient macrophages treated with tumor cell debris was lower than that in WT macrophages (Fig. 4c). HO-1-deficient macrophages treated with tumor cell debris showed decreased mRNA levels of *Il10* compared to the WT macrophages (Fig. 4d). Taken together, these results suggest that HO-1 signaling induced by tumor cell debris represses the M1-like polarization of macrophages in the TME following chemotherapy.

HO-1 inactivation amplifies the therapeutic efficacy of PTX

To determine whether HO-1 inactivation could enhance the therapeutic efficiency of PTX, we used HO-1 KO mice implanted with 4T1 breast cancer cells. We injected PTX into the mice when tumors were grown for 10 days. Notably, the therapeutic efficacy of PTX was increased in HO-1 KO mice compared to the WT mice (Fig. 5a). However, the tumor weight was not that much different between HO-1 WT and KO mice treated with PTX due to the relatively larger size of initial tumors at the time point of PTX injection (Supplemental Fig. S2a and Fig. S2b).

To further confirm the role of HO-1 in the response to PTX, 4T1 tumor cell-implanted mice were injected with PTX and the HO-1 inhibitor, ZnPP. We found that co-treatment of mice with ZnPP and PTX suppressed tumor growth more effectively than PTX treatment alone (Fig. 5b). The pharmacologic inhibition of HO-1 resulted in a further decrease of the tumor weight compared to PTX treatment alone (Supplemental Fig. S2c). In the context of an anti-tumor immune response, sufficient numbers of infiltrating T cells are needed to achieve a favorable clinical outcome [13,41]. In Balb/c mice implanted with 4T1 tumor cells, PTX administration significantly reduced the proportion of $CD8^+$ cytotoxic T lymphocytes, but this was restored by HO-1 inhibition with ZnPP (Fig. 5c).

Discussion

For decades, various anti-tumor therapies have utilized a wide array of strategies in an attempt to eliminate tumors [15]. However such therapies can trigger massive changes in aspects of the immune contexture, including the density, location and composition of tumor-infiltrating immune cells [13,42]. Cytotoxic therapy can shift the TME toward an immunosuppressive microenvironment, so strategies to maintain a durable anti-tumor immune response during chemotherapy are desirable [5,13,35]. In this context, reprogramming the TME to an immunogenic phenotype may potentiate therapeutic efficacy for tumor regression [43].

Tumor cell debris produced during chemotherapy has been shown to stimulate tumor growth, and this is a critical problem for cancer therapy [15,17]. Phosphatidylserine presented on the surface of tumor cell debris can provoke an immunosuppressive condition in TME [19]. A chemotherapy-induced generation of an immunosuppressive TME influences macrophage polarization, which may account for the poor therapeutic response [20,44]. These findings suggest that tumor cell debris generated during chemotherapy undergoes phagocytosis by macrophages, and this inhibits manifestation of the M1-like macrophage phenotype, thereby dampening the anti-tumor immune response. Therefore, chemotherapeutic strategies that focus on killing cancer cells may act as a double-edged sword.

HO-1 plays an important role in the maintenance of homeostasis. However, it has been reported that HO-1 may also promote tumor progression [25]. We found that the tumors initially grown in HO-1 KO mice implanted with 4T1 murine mammary adenocarcinoma cells were larger than those formed in the WT mice while they were shrunken to a greater extent after PTX treatment. We speculate that HO-1 may have a tumor suppressive function in the early stage of carcinogenesis. Upon chemotherapy, however, HO-1 may stimulate the tumor growth. In the TME, TAMs are a major source of HO-1, which mediates immune suppression in breast cancer [26,45]. Here, we demonstrate that engulfed breast tumor cell debris stimulates the HO-1 expression in macrophages and thereby inhibits M1-like macrophage polarization. Conversely, inactivation of HO-1 in macrophages enhances therapeutic efficacy by polarizing them toward the M1-like phenotype.

Impairment of LC3-associated phagocytosis followed by engulfment of dying cancer cells was previously shown to regulate the polarization of macrophages toward the M1-like phenotype [22]. This raises the possibility that tumor cell debris-induced HO-1 overexpression may regulate the immunomodulatory signaling of macrophage polarization via the LC3-associated phagocytosis pathway. Collectively, these results suggest that targeting HO-1 overexpressed in macrophages engulfing tumor cell debris could be a potential strategy to promote chemotherapeutic efficacy by switching macrophages to an immune-stimulatory phenotype.

Potentiation of the immunogenic function of M1-like TAMs is critical for proper T cell activation in the TME [12,46,47]. Typically, M1-like TAMs mediate the influx of T cells through production of T cell chemokines [12,39]. Abundant accumulation of M1-like TAMs and $CD8^+$ T cells in a tumor has been associated with favorable patient outcomes and thus may be a critical component of anti-tumor therapy [42]. Here, the increased proportion of $CD8^+$ T cells was shown in a 4T1 tumor model upon treatment with PTX and a HO-1 inhibitor. Together, these findings suggest that the polarization of TAMs toward the M1-like phenotype

through HO-1 inhibition converts an immunosuppressive TME to an immunogenic one during chemotherapy.

Immune checkpoint blockade therapy (e.g., with anti-CTLA-4 and PD-1), which is a firmly established treatment for cancer, acts against a variety of tumor types by enhancing anti-tumor immunity [41,48]. However, only a small proportion of patients show a clinical response to this therapy, suggesting that other immune-modulatory treatments might be required for better therapeutic outcome [26,41,49]. The failure of immune checkpoint inhibitors is likely to reflect the immunosuppressive nature of the TME [7]. Reprogramming TAMs toward an immune-stimulatory phenotype enhances the activity of immune checkpoint inhibitors [12,14,49]. Thus, it will be worthwhile to determine whether the M1-like TAMs induced by HO-1 inactivation could improve the response to immune checkpoint inhibitors.

In summary, TAM-mediated phagocytosis of breast tumor cell debris diminishes therapeutic efficacy by decreasing the proportion of M1-like TAMs after chemotherapy. Specifically, we reveal that tumor cell debris-induced HO-1 expression in macrophages affects their polarization in the direction of immunosuppression upon chemotherapy (Fig. 6), and that inhibition of HO-1 overexpression in TAMs can create a robust anti-tumor immune response to potentiate the efficacy of chemotherapy.

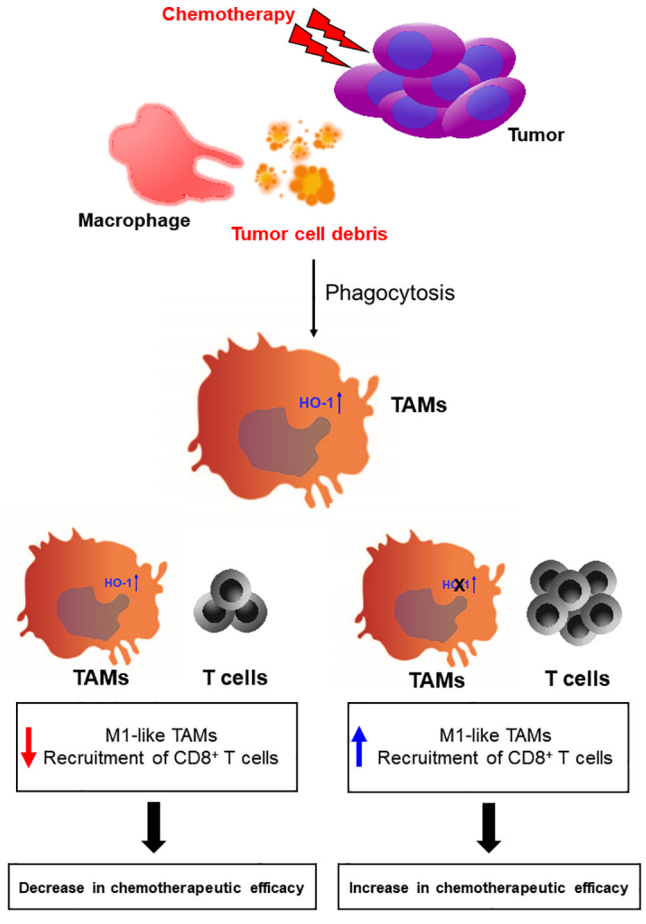

Fig. 6. Schematic representation of the mechanisms underlying TAM-mediated phagocytosis of tumor cell debris in the TME after chemotherapy. Phagocytosis of tumor cell debris upregulates the HO-1 expression of macrophages upon chemotherapy. This overexpression of HO-1 regulates the polarization of TAMs in the TME. Therefore, reprogramming of TAMs by HO-1 inactivation is a potential strategy for improving the response to chemotherapy via enhancement of anti-tumor immunity.

Authors' contributions

SHK designed the research study; SHK, SS, XZ, SYG, and IAM performed the research; SHK, SS, SAP and YJS analyzed the data; SHK and YJS wrote the paper; SAP, SHK, HKN, YSJ and HTC gave technical support.

Declaration of Competing Interest

The authors declare that they have no known competing financial interests or personal relationships that could have appeared to influence the work reported in this paper.

Acknowledgements

The authors thank Prof. Wonshik Han of Seoul National University Hospital for the generous supply of tumor specimens.

Financial support

This work was supported by the Global Core Research Center (GCRC Grant No. 2011-003-0001) and the BK21 Plus Program (10Z20130000017) of the National Research Foundation (NRF) funded from the Ministry of Education, Republic of Korea.

Appendix A. Supplementary data

Supplementary data to this article can be found online at https://doi.org/10.1016/j.neo.2020.08.006.

References

1. Tong CWS, Wu M, Cho WCS, To KKW. Recent advances in the treatment of breast cancer. *Front Oncol* 2018;**8**:227.
2. Du XL, Key CR, Osborne C, Mahnken JD, Goodwin JS. Discrepancy between consensus recommendations and actual community use of adjuvant chemotherapy in women with breast cancer. *Ann Intern Med* 2003;**138**(2):90–7
3. Verma R, Foster RE, Horgan K, Mounsey K, Nixon H, Smalle N, et al. Lymphocyte depletion and repopulation after chemotherapy for primary breast cancer. *Breast Cancer Res* 2016;**18**(1):10.
4. Maman S, Witz IP. A history of exploring cancer in context. *Nat Rev Cancer* 2018;**18**(6):359–76.
5. Hirata E, Sahai E. Tumor microenvironment and differential responses to therapy. *Cold Spring Harbor Perspect Med* 2017;**7**(7).
6. Onyema OO, Decoster L, Njemini R, Forti LN, Bautmans I, De Waele M, et al. Chemotherapy-induced changes and immunosenescence of CD8+ T-cells in patients with breast cancer. *Anticancer Res* 2015;**35**(3):1481–9.
7. Samanta D, Park Y, Ni X, Li H, Zahnow CA, Gabrielson E, et al. Chemotherapy induces enrichment of $CD47^+/CD73^+/PDL1^+$ immune evasive triple-negative breast cancer cells. *Proc Natl Acad Sci USA* 2018;**115**(6):E1239–48.
8. McCoy MJ, Lake RA, van der Most RG, Dick IM, Nowak AK. Post-chemotherapy T-cell recovery is a marker of improved survival in patients with advanced thoracic malignancies. *Br J Cancer* 2012;**107**(7):1107–15.
9. Zhao Y, Zhang C, Gao L, Yu X, Lai J, Lu D, et al. Chemotherapy-induced macrophage infiltration into tumors enhances nanographene-based photodynamic therapy. *Cancer Res* 2017;**77**(21):6021–32.
10. Mantovani A, Marchesi F, Malesci A, Laghi L, Allavena P. Tumour-associated macrophages as treatment targets in oncology. *Nat Rev Clin Oncol* 2017;**14**(7):399–416.
11. Biswas SK, Mantovani A. Macrophage plasticity and interaction with lymphocyte subsets: cancer as a paradigm. *Nat Immunol* 2010;**11**(10):889–96.
12. Baer C, Squadrito ML, Laoui D, Thompson D, Hansen SK, Kiialainen A, et al. Suppression of microRNA activity amplifies IFN-γ-induced macrophage activation and promotes anti-tumour immunity. *Nat Cell Biol* 2016;**18**(7):790–802.

13. Fridman WH, Zitvogel L, Sautes-Fridman C, Kroemer G. The immune contexture in cancer prognosis and treatment. *Nat Rev Clin Oncol* 2017;**14**(12):717–34.
14. Kaneda MM, Messer KS, Ralainirina N, Li H, Leem CJ, Gorjestani S, et al. PI3Kγ is a molecular switch that controls immune suppression. *Nature* 2016;**539**(7629):437–42.
15. Sulciner ML, Serhan CN, Gilligan MM, Mudge DK, Chang J, Gartung A, et al. Resolvins suppress tumor growth and enhance cancer therapy. *J Exp Med* 2018;**215**(1):115–40.
16. Chang YS, Jalgaonkar SP, Middleton JD, Hai T. Stress-inducible gene Atf3 in the noncancer host cells contributes to chemotherapy-exacerbated breast cancer metastasis. *Proc Natl Acad Sci USA* 2017;**114**(34):E7159–68.
17. Chang J, Bhasin SS, Bielenberg DR, Sukhatme VP, Bhasin M, Huang S, et al. Chemotherapy-generated cell debris stimulates colon carcinoma tumor growth via osteopontin. *FASEB J* 33 (1), 2019, 114-125.
18. Roca H, Jones JD, Purica MC, Weidner S, Koh AJ, Kuo R, et al. Apoptosis-induced CXCL5 accelerates inflammation and growth of prostate tumor metastases in bone. *J Clin Invest* 2018;**128**(1):248–66.
19. Kumar S, Calianese D, Birge RB. Efferocytosis of dying cells differentially modulate immunological outcomes in tumor microenvironment. *Immunol Rev* 2017;**280**(1):149–64.
20. Brown JM, Recht L, Strober S. The promise of targeting macrophages in cancer therapy. *Clin Cancer Res* 2017;**23**(13):3241–50.
21. Voss J, Ford CA, Petrova S, Melville L, Paterson M, Pound JD, et al. Modulation of macrophage antitumor potential by apoptotic lymphoma cells. *Cell Death Differ* 2017;**24**(6):971–83.
22. Cunha LD, Yang M, Carter R, Guy C, Harris L, Crawford JC, et al. LC3-associated phagocytosis in myeloid cells promotes tumor immune tolerance. *Cell* 2018;**175**(2):429–41.
23. Gorrini C, Harris IS, Mak TW. Modulation of oxidative stress as an anticancer strategy. *Nat Rev Drug Disc* 2013;**12**(12):931–47.
24. Nitti M, Piras S, Marinari UM, Moretta L, Pronzato MA, Furfaro AL. HO-1 induction in cancer progression: a matter of cell adaptation. *Antioxidants* 2017;**6**(2):29.
25. Na HK, Surh YJ. Oncogenic potential of Nrf2 and its principal target protein heme oxygenase-1. *Free Radical Biol Med* 2014;**67**:353–65.
26. Muliaditan T, Opzoomer JW, Caron J, Okesola M, Kosti P, Lall S, et al. Repurposing tin mesoporphyrin as an immune checkpoint inhibitor shows therapeutic efficacy in preclinical models of cancer. *Clin Cancer Res* 2018;**24**(7):1627–8.
27. Alaoui-Jamali MA, Bismar TA, Gupta A, Szarek WA, Su J, Song W, et al. A novel experimental heme oxygenase-1-targeted therapy for hormone-refractory prostate cancer. *Cancer Res* 2009;**69**(20):8017–24.
28. Metz R, DuHadaway JB, Rust S, Munn DH, Muller AJ, Mautino M, et al. Zinc protoporphyrin-IX stimulates tumor immunity by disrupting the immunosuppressive enzyme indoleamine 2,3-dioxygenase. *Mol Cancer Ther* 2010;**9**(6):1864–71.
29. Di Biase S, Lee C, Brandhorst S, Manes B, Buono R, Cheng CW, et al. Fasting-mimicking diet reduces HO-1 to promote T cell-mediated tumor cytotoxicity. *Cancer Cell* 2016;**30**(1):136–46.
30. Halin Bergstrom S, Nilsson M, Adamo H, Thysell E, Jernberg E, Stattin P, et al. Extratumoral heme oxygenase-1 (HO-1) expressing macrophages likely promote primary and metastatic prostate tumor growth. *PLoS ONE* 2016;**11**(6) e0157280.
31. Hughes R, Qian BZ, Rowan C, Muthana M, Keklikoglou I, Olson OC, et al. Perivascular M2 macrophages stimulate tumor relapse after chemotherapy. *Cancer Res* 2015;**75**(17):3479–91.
32. Pulaski BA, Ostrand-Rosenberg S. Mouse 4T1 breast tumor model. *Curr Protoc Immunol* 2001, Chapter 20:Unit 20.2.
33. Pachynski RK, Scholz A, Monnier J, Butcher EC, Zabel BA. Evaluation of tumor-infiltrating leukocyte subsets in a subcutaneous tumor model. *J Visual Exp* 2015;**98**:52657.
34. Karagiannis GS, Pastoriza JM, Wang Y, Harney AS, Entenberg D, Pignatelli J, et al. Neoadjuvant chemotherapy induces breast cancer metastasis through a TMEM-mediated mechanism. *Sci Transl Med* 2017;**9**(397).
35. Ruffell B, Chang-Strachan D, Chan V, Rosenbusch A, Ho CM, Pryer N, et al. Macrophage IL-10 blocks CD8+ T cell-dependent responses to chemotherapy by suppressing IL-12 expression in intratumoral dendritic cells. *Cancer Cell* 2014;**26**(5):623–37.
36. Rugo HS, Barry WT, Moreno-Aspitia A, Lyss AP, Cirrincione C, Leung E, et al. Randomized phase III trial of paclitaxel once per week compared with nanoparticle albumin-bound nab-paclitaxel once per week or ixabepilone with bevacizumab as first-line chemotherapy for locally recurrent or metastatic breast cancer: CALGB 40502/NCCTG N063H (Alliance). *J Clin Oncol* 2015;**33**(21):2361–9.
37. Cassetta L, Noy R, Swierczak A, Sugano G, Smith H, Wiechmann L, et al. Isolation of mouse and human tumor-associated macrophages. *Adv Exp Med Biol* 2016;**899**:211–29.
38. Dijkgraaf EM, Heusinkveld M, Tummers B, Vogelpoel LT, Goedemans R, Jha V, et al. Chemotherapy alters monocyte differentiation to favor generation of cancer-supporting M2 macrophages in the tumor microenvironment. *Cancer Res* 2013;**73**(8):2480–92.
39. Mantovani A, Allavena P. The interaction of anticancer therapies with tumor-associated macrophages. *J Exp Med* 2015;**212**(4):435–45.
40. Naito Y, Takagi T, Higashimura Y. Heme oxygenase-1 and anti-inflammatory M2 macrophages. *Arch Biochem Biophys* 2014;**564**:83–8.
41. Spranger S, Gajewski TF. Impact of oncogenic pathways on evasion of antitumour immune responses. *Nat Rev Cancer* 2018;**18**(3):139–47.
42. Becht E, Giraldo NA, Dieu-Nosjean MC, Sautes-Fridman C, Fridman WH. Cancer immune contexture and immunotherapy. *Curr Opin Immunol* 2016;**39**:7–13.
43. Binnewies M, Roberts EW, Kersten K, Chan V, Fearon DF, Merad M, et al. Understanding the tumor immune microenvironment (TIME) for effective therapy. *Nat Med* 2018;**24**(5):541–50.
44. Ubil E, Caskey L, Holtzhausen A, Hunter D, Story C, Earp HS. Tumor-secreted Pros1 inhibits macrophage M1 polarization to reduce antitumor immune response. *J Clin Invest* 2018;**128**(6):2356–69.
45. Arnold JN, Magiera L, Kraman M, Fearon DT. Tumoral immune suppression by macrophages expressing fibroblast activation protein-α and heme oxygenase-1. *Cancer Immunol Res* 2014;**2**(2):121–6.
46. Daley D, Mani VR, Mohan N, Akkad N, Pandian G, Savadkar S, et al. NLRP3 signaling drives macrophage-induced adaptive immune suppression in pancreatic carcinoma. *J Exp Med* 2017;**214**(6):1711–24.
47. Medler TR, Cotechini T, Coussens LM. Immune response to cancer therapy: mounting an effective antitumor response and mechanisms of resistance. *Trends Cancer* 2015;**1**(1):66–75.
48. Sharma P, Allison JP. The future of immune checkpoint therapy. *Science (New York, NY).* 2015;**348**(6230):56–61.
49. Georgoudaki AM, Prokopec KE, Boura VF, Hellqvist E, Sohn S, Ostling J, et al. Reprogramming tumor-associated macrophages by antibody targeting inhibits cancer progression and metastasis. *Cell Rep* 2016;**15**(9):2000–11.